Diagnostic accuracy of ultrasound-guided attenuation parameter as a noninvasive test for steatosis in non-alcoholic fatty liver disease

Hidekatsu Kuroda[1] · Tamami Abe[1] · Yudai Fujiwara[1] · Tomoaki Nagasawa[1] · Yasuhiro Takikawa[1]

Abstract

The purpose of this study was to evaluate the diagnostic accuracy of the ultrasound-guided attenuation parameter (UGAP) using the LOGEQ E10 for hepatic steatosis in non-alcoholic fatty liver disease (NAFLD) patients and directly compare UGAP with attenuation imaging (ATI) and controlled attenuation parameter (CAP). We prospectively analyzed 105 consecutive patients with NAFLD who underwent UGAP, ATI, CAP, and liver biopsy on the same day between October 2019 and April 2021. The diagnostic ability of the UGAP-determined attenuation coefficient (AC) was evaluated using receiver operating characteristic (ROC) curve analysis, and its correlation with ATI-determined AC values or CAP values was investigated. The success rate of UGAP was 100%. The median IQR/med obtained by UGAP was 4.0%, which was lower than that of ATI and CAP ($P < 0.0001$). The median ACs obtained by UGAP for grades S0 (control), S1, S2, and S3 were 0.590, 0.670, 0.750, and 0.845 dB/cm/MHz, respectively, demonstrating a stepwise increase with increasing hepatic steatosis severity ($P < 0.0001$). The areas under the ROC curve of UGAP for identifying $\geq$ S1, $\geq$ S2, and S3 were 0.890, 0.906, and 0.912, respectively, which were significantly better than the results obtained with CAP for identifying S3. Furthermore, the correlation coefficient between UGAP-AC and ATI-AC values was 0.803 ($P < 0.0001$), indicating a strong relationship. Our results indicate that UGAP has high diagnostic accuracy for detecting and grading hepatic steatosis in patients with NAFLD.

Keywords Ultrasound-guided attenuation parameter · Hepatic steatosis · Non-alcoholic fatty liver disease · Attenuation coefficient

Introduction

Non-alcoholic fatty liver disease (NAFLD) is considered the most common chronic liver disease worldwide, with a dramatic global increase in prevalence similar to that of obesity and diabetes mellitus [1, 2, 3]. NAFLD is a spectrum of diseases ranging from simple hepatic steatosis to non-alcoholic steatohepatitis (NASH), advanced fibrosis, cirrhosis, and hepatocellular carcinoma. Histologically, the liver is considered steatotic when more than 5% of hepatocytes in a tissue section stained with hematoxylin and eosin display macrovesicular steatosis [4, 5]. Hepatic steatosis is a common histological feature among patients with chronic liver disease, and its coexistence can accelerate fibrosis and reduce treatment response [6, 7]. Therefore, accurate detection and grading of hepatic steatosis are essential for clinical decision making and prognosis estimation.

Liver biopsy (LB) remains the reference standard for diagnosing and grading hepatic steatosis, fibrosis, and inflammation [8]. However, LB is invasive and subject to sampling error and intra- and inter-observer variability [9, 10]. Moreover, magnetic resonance imaging (MRI)-based methods are expensive; therefore, it is impractical for screening large populations and is not widely available [11]. Conventional B-mode abdominal ultrasonography is the most widely used technique for detecting liver steatosis [12]. However, it has low sensitivity, especially when there is less than 20% hepatic fat infiltration [13].

Recently, the controlled attenuation parameter (CAP), a physical parameter acquired with the FibroScan® (Echosens, Paris, France) device, has been widely used to assess

✉ Hidekatsu Kuroda
    hikuro@iwate-med.ac.jp

1 Division of Hepatology, Department of Internal Medicine, Iwate Medical University, Nishitokuta 2-1-1, Yahaba-cho, Shiwa-gun, Iwate 028-3694, Japan

steatosis [14–18]. However, the CAP technique can only be performed in A-mode [19]. Since the region of interest is not visualized during the measurement, artifacts and areas of heterogeneous liver parenchyma cannot be avoided with this method. In contrast, the ultrasound-guided attenuation parameter (UGAP) measures the attenuation coefficient (AC) (dB/cm/MHz) of the B-mode ultrasonic signal via general ultrasonography [19–22]. The UGAP was embedded by GE Healthcare (Wauwatosa, WI, USA) into the LOGIQ E10 ultrasound device [23]. However, there are limited reports about the ability of UGAP to diagnose and grade hepatic steatosis in patients with NAFLD, and most of these are based on the results of an offline analysis of the radiofrequency-based ultrasound echo signals using a dedicated prototype software program with MATLAB (MathWorks, Inc., Natick, MA, USA). Moreover, several companies market ultrasound-based attenuation imaging devices, such as Attenuation Imaging (ATI; Canon Medical Systems, Otawara, Japan) [24–28]. A few studies have directly compared the results obtained using various ultrasound devices in the same patient. Consequently, there is no consensus on the evaluation of data derived from each device, leading to some confusion among physicians and sonographers.

Therefore, we evaluated the accuracy of UGAP assessed using LOGIQ E10 for grading hepatic steatosis in patients with NAFLD and directly compared it with the diagnostic ability of ATI and CAP performed on the same day.

Materials and methods

Patients

This cross-sectional, prospective study included patients evaluated at the Iwate Medical University Hospital, Iwate, Japan. The cohort comprised 113 consecutive patients with NAFLD who underwent UGAP, ATI, CAP, and LB between October 2019 and April 2021. For each patient, all procedures were performed on the same day. The inclusion criteria were the ability to provide informed consent and age between 18 and 80 years. NAFLD diagnosis was based on the presence of steatosis in the LB specimen. The exclusion criteria were alcohol consumption (consuming ≥ 40 g alcohol per day for men and ≥ 20 g per day for women in the preceding 12 months) and other liver diseases, such as chronic hepatitis, drug use associated with fatty liver, or untreated hypothyroidism [29]. The control group comprised 20 participants, all of whom had normal liver enzyme levels and no evidence of fatty liver, with mean age and sex ratios matched to those of the NAFLD group. We determined that there was no evidence of fatty liver in cases without typical ultrasonographic findings, such as a bright liver pattern, liver–kidney contrast, and poor visualization of the portal vein wall or diaphragm.

UGAP

The UGAP, ATI, and CAP assessments were performed independently by one of two experienced radiologists in control participants and patients with NAFLD on the same day as LB. The radiologists were blinded to the patients' histological and clinical data. UGAP measurements were performed using a LOGIQ E10 ultrasound device (GE Healthcare) with a C1-6-D convex array probe at a frequency of 4.0 MHz. All measurements were taken in the right liver lobe (segment 5) by an intercostal approach, during short breath holds, with the patient in the fasting state (> 4 h), in a supine position, and with the right arm in maximum abduction. The liver target area was visualized using conventional real-time B-mode imaging. A large attenuation map, automatically adjusted by the system, was positioned in the right liver lobe in a homogenous area (Fig. 1a) free
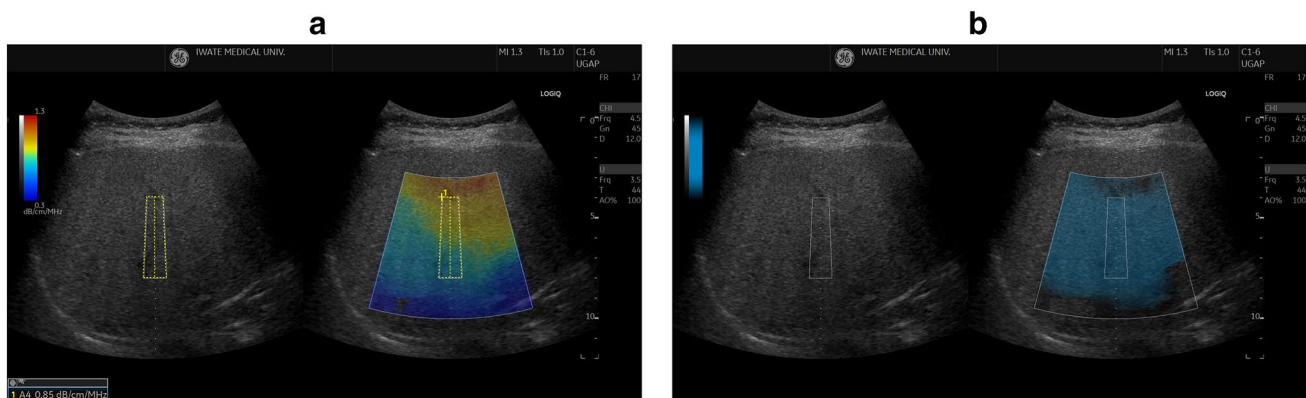

Fig. 1 Ultrasound-guided attenuation parameter (UGAP). A large attenuation map, automatically adjusted by the system, was positioned in the right liver lobe in a homogenous area free of large ves-sels (**a**). Using the quality map, the best image was selected to acquire the attenuation coefficient measurement (**b**)

of large vessels. Using the quality map, the best image was selected to acquire the attenuation coefficient measurements (Fig. 1b). A reliable AC was defined as more than five valid shots, a success rate of at least 60%, and an interquartile range/median (IQR/med) < 30%. The AC is expressed in dB/cm/MHz.

ATI

The measurement principles and methods, including the regions of interest, of ATI have been previously described [24, 30]. Gray-scale ultrasonography and ATI examinations were performed using a diagnostic ultrasound device (Aplio i800; Canon Medical Systems Corp., Otawara, Tochigi, Japan) with a convex probe (1–8 MHz) in patients who had fasted for at least 4 h. The median value of five consecutive ATI measurements during a single examination session was used for the statistical analysis. A reliable AC was defined as more than five valid shots, a success rate of at least 60%, and an IQR/med < 30% of the median AC value.

CAP

CAP measurements were performed using the FibroScan® 502 Touch with a 3.5 MHz M probe (Echosens, Paris, France). CAP measurements were performed as previously described [31, 32]. The tip of the ultrasound probe was placed on the skin in an intercostal space overlying the right lobe of the liver (segment 5). The result was the median of ≥ 10 valid measurements. Measurements were taken at a depth of 25–65 mm, and only valid measurements were included based on the internal algorithm of the device. Reliability was defined as ≥ 10 valid measurements, IQR/med < 30%, and success rate > 60%.

Histological evaluation

Echo-assisted LB samples were obtained using a 14-gauge needle biopsy kit. An adequate LB sample was defined as being > 15 mm in length and having > 6 portal tracts visualized under microscopy. LB specimens were fixed in formalin, embedded in paraffin, stained with hematoxylin/eosin and Gomori trichrome for fibrosis evaluation, and assessed by two experienced pathologists blinded to each other's readings and patients' clinical data. Macrovesicular steatosis affecting ≥ 5% of hepatocytes was observed in all patients with NAFLD. NASH was diagnosed using the fatty liver inhibition of progression algorithm and steatosis, activity, and fibrosis score [33]. In addition, steatosis (1–3), ballooning (0–2), lobular inflammation (0–3), and fibrosis (0–4) were scored using the NASH Clinical Research Network Scoring System.

Statistical analysis

Statistical analyses were performed using SPSS version 23 (IBM, Armonk, NY, USA) and XLSTAT 2019 (Microsoft Corp., WA, USA). Data are presented as means ± standard deviations (normally distributed data) or as medians (25th–75th percentiles) (non-normally distributed data). The correlations between the measurement results were assessed using Spearman's rank correlation coefficient. The correlation coefficient (r) was classified as almost none ($r < 0.2$), weak ($r = 0.2$–0.4), moderate ($r = 0.4$–0.7), or strong ($r \geq 0.7$). Similarly, we used the Kruskal–Wallis test to compare the measurement results of the different steatosis grades. Post-hoc multiple comparisons were performed using the Mann–Whitney U test with Bonferroni correction. Receiver operating characteristic (ROC) curves were constructed, and the trapezoidal rule was used to calculate the area under the ROC curve (AUROC). Differences in the diagnostic accuracies of UGAP, ATI, and CAP were evaluated by comparing the AUCs (method of Delong et al. for correlated data) [34]. The optimal cutoff points for predicting different steatosis grades were identified based on the highest Youden index. Sensitivity, specificity, positive predictive value, and negative predictive value were calculated using cutoff values obtained from ROC curves.

Results

Patients' baseline characteristics

In total, 117 patients with NAFLD who underwent UGAP, ATI, CAP, and LB assessments were enrolled. Six patients were excluded due to disqualified biopsy specimens ($n = 3$) and excessive alcohol consumption ($n = 3$). The UGAP, ATI, and CAP success rates were 100% (111/111), 100% (111/111), and 94.6% (105/111), respectively. CAP failed in six patients (body mass index > 30 kg/m^2, six patients; inability to optimally perform a breath-hold, six patients). Statistical analysis included 105 patients (94.6%) (Fig. 2). Table 1 summarizes the characteristics of the included patients with NAFLD and 20 control participants.

Comparison of IQR/median between UGAP, ATI, and CAP

The median IQR/med obtained using UGAP, ATI, and CAP were 4.0%, 7.5%, and 10.8%, respectively. The median IQR/med was significantly lower for UGAP than for ATI and CAP ($P < 0.0001$). Moreover, it was significantly lower for ATI than for CAP (Table 2).

NAFLD patients who underwent UGAP, ATI, CAP, and LB
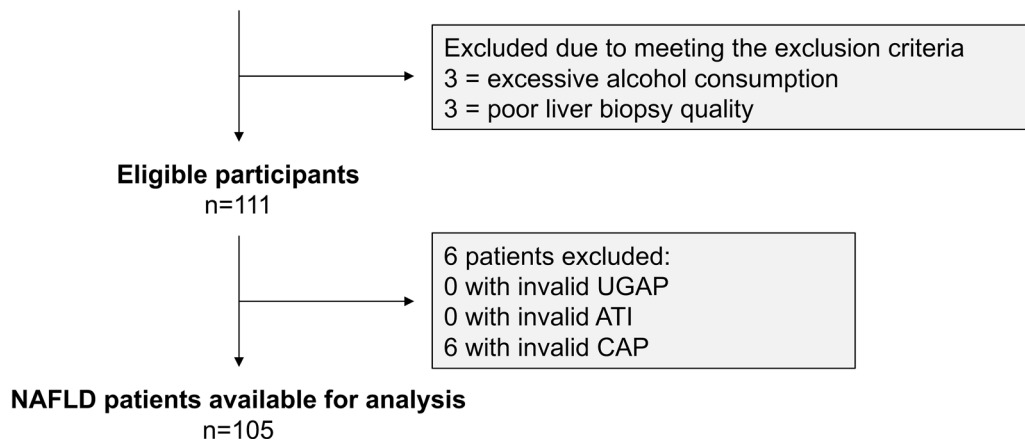（Oct 2019 - Apr 2021）
n=117

Excluded due to meeting the exclusion criteria
3 = excessive alcohol consumption
3 = poor liver biopsy quality

Eligible participants
n=111

6 patients excluded:
0 with invalid UGAP
0 with invalid ATI
6 with invalid CAP

NAFLD patients available for analysis
n=105

Fig. 2 Flow diagram of the study population

Table 1 Baseline characteristics of control participants and patients with NAFLD

Variables	Control	NAFLD
n	20	105
Sex (male/female)	10/10	53/52
Mean age (years)	54.3 ± 16.1	53.9 ± 17.7
BMI (kg/m^2)	24.1 [19.8–23.2]	29.8 [25.6–34.1]
Skin–liver capsule distance (mm)	17.5 [13.3–18.5]	21.5 [18.4–25.2]
T.Bil (mg/dL)	0.6 [0.5–0.9]	0.7 [0.5–0.9]
AST (U/L)	21.5 [17.0–24.0]	34.5 [23.8–48.5]
ALT (U/L)	22.1 [17.5–25.0]	42.1 [25.8–76.8]
Alb (g/dL)	4.5 [4.2–4.7]	4.2 [3.8–4.4]
GGT (U/L)	23.0 [12.5–30.3]	47.5 [25.8–89.3]
FPG (mg/dL)	92.0 [91.0–98.8]	108.5 [92.8–141.5]
IRI (μU/mL)	6.6 [4.3–8.5]	13.1 [8.5–23.9]
HDL-C (mg/dL)	63.0 [48.5–80.7]	45.5 [38.0–57.3]
TG (mg/dL)	85.7 [56.5–118.5]	131.5 [92.3–164.8]
Plt (×10^4/mm^3)	23.7 [18.8–25.7]	21.5 [16.9–25.1]
NAFL/NASH		22/83
Fibrosis stage, F0/F1/F2/F3/F4		23/39/16/16/11
Steatosis grade S0/S1/S2/S3		51/28/26
Lobular inflammation grade, A0/A1/A2/A3		22/57/20/6
Ballooning grade, B0/B1/B2		31/52/19/3

The values are shown as the mean ± standard deviation or the median [25–75th percentile]

Alb albumin, *ALT* alanine aminotransferase, *AST* aspartate aminotransferase, *BMI* body mass index, *FPG* fasting plasma glucose, *GGT* gamma-glutamyl transferase, *HDL-C* HDL cholesterol, *IRI* immunoreactive insulin, *NAFL* non-alcoholic fatty liver, *NAFLD* non-alcoholic fatty liver disease, *NASH* non-alcoholic steatohepatitis, *Plt* platelet count, *T.Bil* total bilirubin, *TG* triglyceride

Hepatic steatosis assessment in NAFLD using UGAP, ATI, and CAP

AC and CAP values were measured using UGAP, ATI, and CAP in patients with NAFLD to assess the hepatic steatosis grade. Median ACs obtained with UGAP for grades S0 (control), S1, S2, and S3 were 0.590, 0.670, 0.750, and 0.845 dB/cm/MHz, respectively, demonstrating a stepwise increase with increasing hepatic steatosis severity ($P < 0.0001$). Statistically significant differences

Table 2 IQR/med obtained by UGAP, ATI, and CAP

Modalities	IQR/med
UGAP	4.0 [2.3–6.2]*, **
ATI	7.5 [5.8–10.6]**
CAP	10.8 [7.1–13.3]

The values are shown as the median [25–75th percentile]

ATI attenuation imaging, *CAP* controlled attenuation parameter, *IQR/med* interquartile range/median, *UGAP* ultrasound-guided attenuation parameter

*$P < 0.001$ (compared with ATI)

**$P < 0.001$ (compared with CAP)

were observed between groups (Fig. 3a). Median ACs obtained with ATI for these grades were 0.600, 0.670, 0.810, and 0.905 dB/cm/MHz, respectively, demonstrating a stepwise increase with increasing hepatic steatosis severity ($P < 0.0001$). In addition, statistically significant differences were observed between groups (Fig. 3b). Median CAP values for these grades were 209.0, 255.0, 299.5, and 320.0 dB/m, respectively, demonstrating a stepwise increase with increasing hepatic steatosis severity ($P < 0.0001$). However, no statistically significant differences were observed between grades S2 and S3 (Fig. 3c). Figure 4 shows a typical image of the quality map and attenuation map for each hepatic steatosis grade.

Performance characteristics of UGAP, ATI, and CAP for the determination of steatosis grade

The optimal cutoff values for the sensitivity, specificity, positive predictive value, and negative predictive value of UGAP, ATI, and CAP for hepatic steatosis grades $\geq$ S1, $\geq$ S2, and S3 are summarized in Table 3. The AUROCs of UGAP for the prediction of steatosis grades $\geq$ S1, $\geq$ S2, and S3 were 0.890 (95% confidence interval (CI) 0.862–0.963), 0.906 (95% CI 0.854–0.957), and 0.912 (95% CI 0.862–0.953), respectively (Fig. 5a). The AUROCs of ATI for these grades were 0.876 (95% CI 0.811–0.942), 0.883 (95% CI 0.829–0.938), and 0.908 (95% CI 0.856–0.959), respectively (Fig. 5b). The AUROCs of CAP for these grades were 0.847 (95% CI 0.780–0.913), 0.866 (95% CI 0.804–0.929), and 0.842 (95% CI 0.774–0.909), respectively (Fig. 5c). AUROCs were higher for UGAP than for ATI and CAP for all grades. In addition, the AUROCs were significantly higher for UGAP and ATI than for CAP in the diagnosis of grade S3 ($P = 0.027$ and $P = 0.028$, respectively).

Correlation of measurement results between UGAP, ATI, and CAP

Figure 6a shows the correlation between UGAP and ATI measurement results, where the r value was 0.803 ($P < 0.0001$), indicating a strong relationship. Figure 6b shows the correlation between UGAP and CAP measurement results, where the r value was 0.681 ($P < 0.0001$), indicating a moderate relationship. Figure 6c shows the correlation between ATI and CAP measurement results, where the r value was 0.694 ($P < 0.0001$), indicating a moderate relationship.
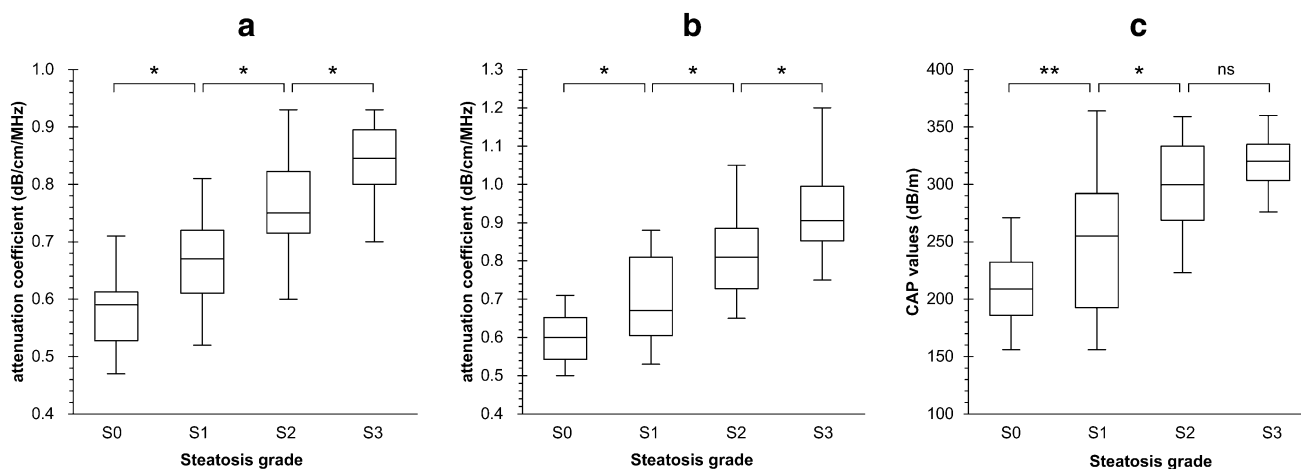

Fig. 3 Attenuation coefficients (ACs) and controlled attenuation parameter (CAP) values distributions for different steatosis grades. ACs and CAP values demonstrated a stepwise increase with increasing hepatic steatosis severity. (**a**) UGAP; (**b**) attenuation imaging (ATI); (**c**) CAP. *$P < 0.01$, **$P < 0.05$. *Ns* not significant
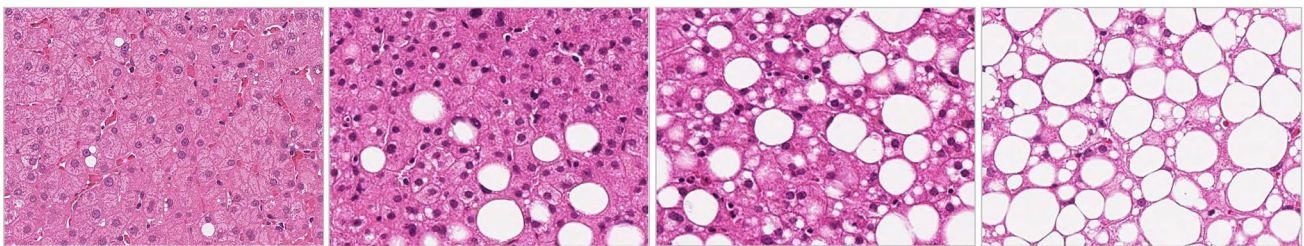
UGAP: Quality map

UGAP: Attenuation map

0.58 dB/cm/MHz   0.67 dB/cm/MHz   0.76 dB/cm/MHz   0.84 dB/cm/MHz
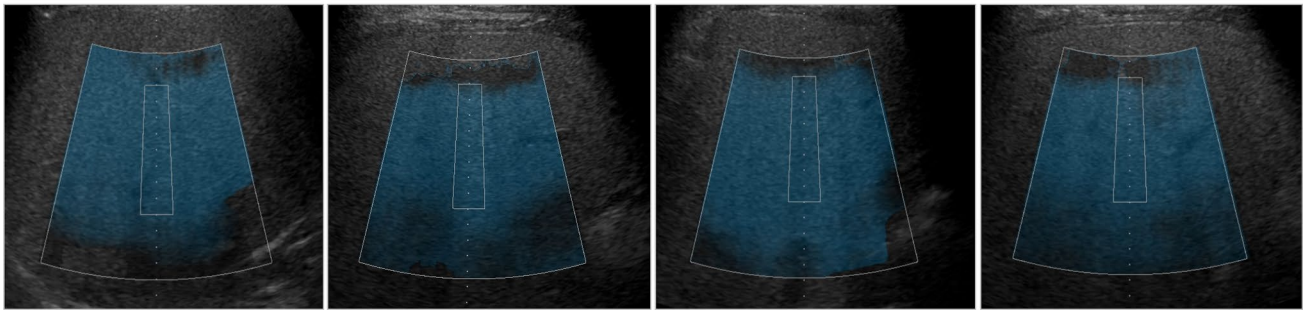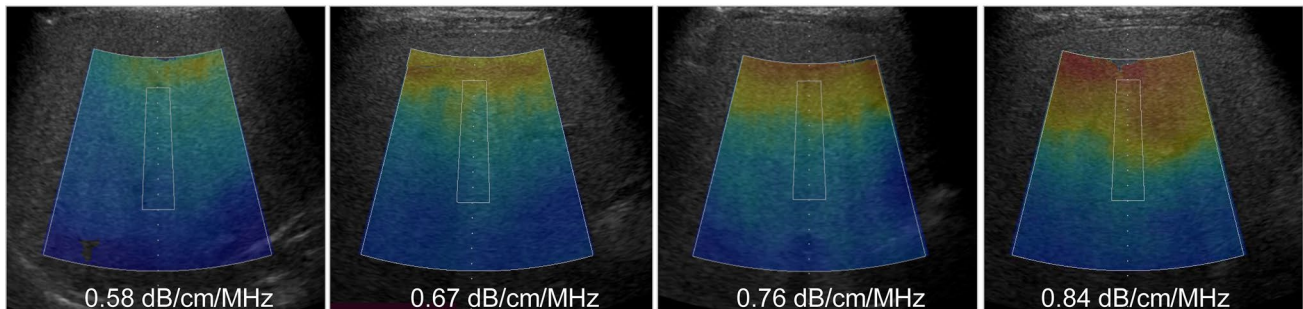
H&E stain

Steatosis grade 0   **Steatosis grade 1**   **Steatosis grade 2**   **Steatosis grade 3**

Fig. 4 Typical images of the quality map and attenuation map for each hepatic steatosis grade

Discussion

The prevalence of NAFLD is increasing in line with obesity, with an estimated global prevalence of 25% [3, 35, 36]. NAFLD leads to increased cardiovascular events, whereas NASH may lead to liver cirrhosis or hepatocellular carcinoma [36, 37]. Therefore, it is crucial to establish an accurate, noninvasive, and objective hepatic steatosis index for NAFLD screening and follow-up.

In this study, we focused on the diagnostic ability of UGAP, implemented using the LOGIQ E10, for hepatic steatosis in NAFLD patients. To our knowledge, this is the first prospective cohort study to evaluate the diagnostic ability of UGAP with LOGIQ E10 with reference to LB results in patients with NAFLD. We observed that UGAP had high diagnostic accuracy for detecting hepatic steatosis in patients with NAFLD.

In previously published reports, Fujiwara et al. reported excellent feasibility of UGAP for liver steatosis quantification (success rate: 100%) [19]. Another report showed that the feasibility of UGAP was very high (success rate: 100%, 98.8%) [22, 23] (Table 4). In this prospective study, the success rates for UGAP, ATI, and CAP were 100%, 100%, 94.6%, respectively. A large meta-analysis showed that CAP values were affected by pathogenesis, body mass index, and diabetes [15]. The reason for failure with CAP in our study was body mass index ≥ 30, as in the meta-analysis. UGAP and ATI can be performed under B-mode guidance, whereas CAP requires A-mode guidance. B-mode guidance enables the visual confirmation of the part to be measured, and factors that affect measurements, such as blood vessels and extrahepatic structures, can be easily excluded. In addition, UGAP had less variability statistically in measurements than the other modalities. UGAP is equipped with a multiple-mode that allows multiple data to be acquired with a single

Table 3 Diagnostic accuracy of UGAP, ATI, and CAP for the diagnosis of steatosis grade

	≥ S1 (95% Cl)			≥ S2 (95% Cl)			S3 (95% Cl)		
	UGAP	ATI	CAP	UGAP	ATI	CAP	UGAP	ATI	CAP
AUROC	0.890	0.876	0.847	0.906	0.883	0.866	0.912*	0.908*	0.842
	(0.862–0.963)	(0.811–0.942)	(0.780–0.913)	(0.854–0.957)	(0.829–0.938)	(0.804–0.929)	(0.862–0.953)	(0.856–0.959)	(0.774–0.909)
Cutoff value	0.620	0.640	246	0.720	0.710	274	0.750	0.750	287
Sensitivity	0.848	0.819	0.762	0.815	0.889	0.852	0.923	0.885	0.923
	(0.765–0.905)	(0.733–0.881)	(0.671–0.833)	(0.689–0.897)	(0.773–0.951)	(0.732–0.925)	(0.745–0.988)	(0.700–0.967)	(0.745–0.988)
Specificity	0.800	0.750	0.950	0.845	0.676	0.732	0.798	0.808	0.687
	(0.577–0.923)	(0.526–0.890)	(0.743–1.000)	(0.741–0.912)	(0.560–0.773)	(0.618–0.822)	(0.707–0.866)	(0.718–0.874)	(0.589–0.770)
PPV	0.957	0.945	0.988	0.800	0.676	0.708	0.548	0.548	0.436
NPV	0.500	0.441	0.432	0.857	0.889	0.867	0.964	0.964	0.971

AUROC area under receiver the operating curve, *ATI* attenuation imaging, *CAP* controlled attenuation parameter, *CI* confidence interval, *NPV* negative predictive value, *PPV* positive predictive value, *UGAP* ultrasound-guided attenuation parameter
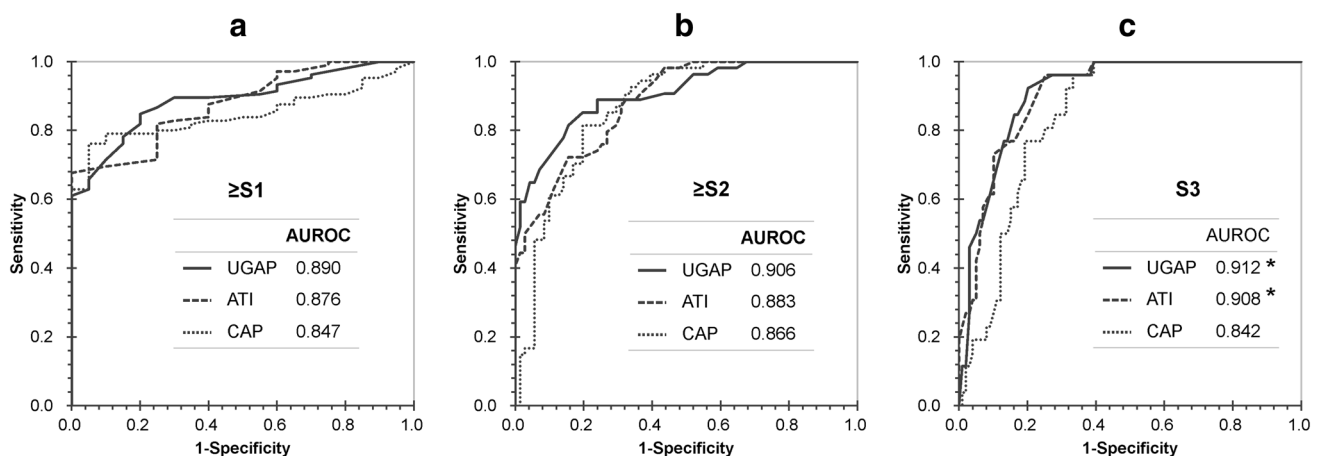
*$P < 0.05$ (compared with CAP)

Fig. 5 Receiver operating characteristic curves for UGAP, ATI, and CAP in the diagnosis of hepatic steatosis. (**a**) ≥ S1 (≥ 5%); (**b**) ≥ S2 (≥ 34%); (**c**) S3 (≥ 67%). The area under the receiver operating characteristic curve (AUROC) was significantly higher for UGAP and TAI than for CAP in the prediction of grade S3 ($P = 0.027$ and $P = 0.028$, respectively)

breath-hold. Moreover, the mobility of the measurement ROI is more limited than ATI. The effect of multiple-mode and limitation of the mobility of the measurement ROI on measurement accuracy remains unclear and should be explored further in future analyses.

In this study, we compared the performance characteristics of UGAP, ATI, and CAP for grading steatosis. The main strength of our study is that it directly compared hepatic steatosis determined using AC and CAP values based on three different ultrasound devices, with all measurements in each patient performed on the same day. A steady stepwise increase in AC and CAP values was observed with increasing severity of steatosis using UGAP, ATI, and CAP.

The AUROC was higher for UGAP than for ATI and CAP in the determination of all grades. In addition, the AUCs were significantly higher for UGAP and ATI than for CAP in the diagnosis of grade S3. From this result, we assume that B-mode image-guided measurements (UGAP and ATI) would have an advantage over A-mode image-guided measurements (CAP), especially in the diagnosis of steatosis grade S3.

The correlation coefficients between AC values from UGAP and ATI were over 0.8, indicating a strong relationship. However, the correlation coefficients between CAP and UGAP and between CAP and ATI were 0.681 and 0.694, respectively. Actual measurements usually fluctuate
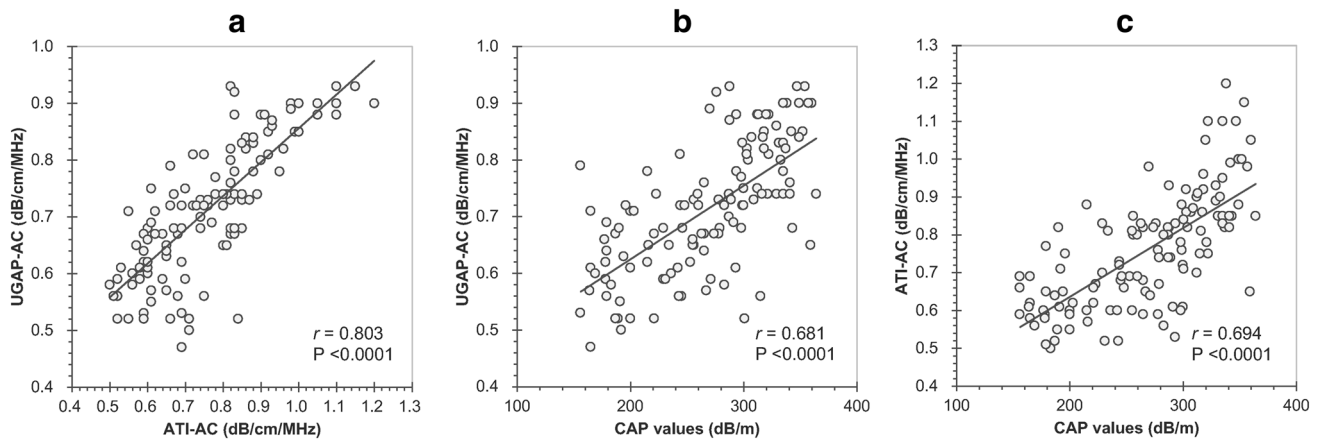
Fig. 6 Correlation of measurement results between UGAP, ATI, and CAP. (**a**) UGAP and ATI; (**b**) UGAP and CAP; (**c**) ATI and CAP

Table 4 Performance of UGAP to diagnose steatosis in patients with chronic liver disease

Author	No. of patients	Etiology	Ultrasonic device	Reference	Success rates	≥ S1		≥ S2		S3	
						Cutoff	AUROC	Cutoff	AUROC	Cutoff	AUROC
Fujiwara [19]	163	Mixed	LOGIQ E9	Liver biopsy	100% (172/172)	0.530	0.900	0.600	0.950	0.650	0.959
Tada [21]	608	Mixed	LOGIQ E9	MRI-PDFF	ND	NT	NT	NT	NT	NT	NT
Tada [20]	126	Mixed	LOGIQ E9	MRI-PDFF	ND	0.603	0.922	0.694	0.874	0.694	0.892
Kuroda [22]	202	NAFLD	LOGIQ E9	Liver biopsy	100% (214/214)	0.493	0.891	0.654	0.909	0.691	0.924
Bende F (23)	177	Mixed	LOGIQ E10	CAP	98.8% (177/179)	0.550	0.830	0.660	0.900	0.700	0.910

AUROC area under receiver the operating curve, *AUROC* area under the receiver operating characteristic, *CAP* controlled attenuation parameter, *MRI* magnetic resonance imaging, *NAFLD* nonalcoholic fatty liver disease, *NT* not tested, *PDFF* proton density fat fraction, *Ud* undescribed, *UGAP* ultrasound-guided attenuation parameter

differently with these types of measurements in biological science; however, the validity of the measurements is supported when there is a strong correlation between the results using different devices. From this perspective, the fact that this study revealed a high correlation between UGAP and ATI, which can be performed under B-mode guidance, is of great significance.

In this study, the diagnostic accuracy of UGAP was excellent, similar to that reported in previous studies. Table 4 shows the performance of UGAP in diagnosing steatosis in patients with chronic liver disease based on previous reports. In most reports published to date, the ultrasonic device used was the LOGIQ E9. Moreover, the etiologies of chronic liver disease varied among subjects, and the references were similarly diverse, such as LB, MRI-PDFF, and CAP. Therefore, the diagnostic ability for all steatosis grades ranged from 0.830 to 0.959, showing generally high diagnostic ability; however, these were all single-center studies, and the numbers of cases were limited. In this regard, the first large-scale multicenter observational study in Japan to evaluate the accuracy of UGAP

in assessing hepatic steatosis in chronic liver disease was initiated in 2020 (UMIN000041196). Based on the results of this multicenter study, it will be necessary to accumulate evidence worldwide in the future.

This study has several limitations, the first of which is the relatively small number of patients. Hence, larger scale prospective clinical studies in multiple countries are needed to confirm our findings. Second, no validation study was performed; thus, future investigations should include validation studies. Third, an ultrasound device is required for UGAP assessment; however, its application is limited by the high cost of the equipment and the need for well-trained operators. Thus, a study design that includes such cases should be considered in future studies.

In conclusion, our findings suggest that UGAP is superior in diagnosing steatosis in patients with NAFLD.

Declarations

References

1. Younossi ZM, Koenig AB, Abdelatif D, et al. Global epidemiology of nonalcoholic fatty liver disease-meta-analytic assessment of prevalence, incidence, and outcomes. Hepatology. 2016;64:73–84.

2. Asrani SK, Devarbhavi H, Eaton J, et al. Burden of liver diseases in the world. J Hepatol. 2019;70:151–71.

3. Younossi ZM. Non-alcoholic fatty liver disease—a global public health perspective. J Hepatol. 2019;70:531–44.

4. Kleiner DE, Brunt EM, Van Natta M, et al. Design and validation of a histological scoring system for nonalcoholic fatty liver disease. Hepatology. 2005;41:1313–21.

5. Brunt EM, Tiniakos DG. Histopathology of nonalcoholic fatty liver disease. World J Gastroenterol. 2010;16:5286–96.

6. Asselah T, Rubbia-Brandt L, Marcellin P, et al. Steatosis in chronic hepatitis C: why does it really matter? Gut. 2006;55:123–30.

7. Perumalswami P, Kleiner DE, Lutchman G, et al. Steatosis and progression of fibrosis in untreated patients with chronic hepatitis C infection. Hepatology. 2006;43:780–7.

8. Rockey DC, Caldwell SH, Goodman ZD, et al. Liver biopsy. Hepatology. 2009;49:1017–44.

9. Vuppalanchi R, Unalp A, Van Natta ML, et al. Effects of liver biopsy sample length and number of readings on sampling variability in nonalcoholic fatty liver disease. Clin Gastroenterol Hepatol. 2009;7:481–6.

10. Regev A, Berho M, Jeffers LJ, et al. Sampling error and intraobserver variation in liver biopsy in patients with chronic HCV infection. Am J Gastroenterol. 2002;97:2614–8.

11. Vilar-Gomez E, Lou Z, Kong N, Vuppalanchi R, et al. Cost effectiveness of different strategies for detecting cirrhosis in patients with nonalcoholic fatty liver disease based on United States health care system. Clin Gastroenterol Hepatol. 2020;18:2305-14.e2312.

12. Hamaguchi M, Kojima T, Itoh Y, et al. The severity of ultrasonographic findings in nonalcoholic fatty liver disease reflects the metabolic syndrome and visceral fat accumulation. Am J Gastroenterol. 2007;102:2708–15.

13. Dasarathy S, Dasarathy J, Khiyami A, et al. Validity of real time ultrasound in the diagnosis of hepatic steatosis: a prospective study. J Hepatol. 2009;51:1061–7.

14. Chan WK, Nik Mustapha NR, Mahadeva S. Controlled attenuation parameter for the detection and quantification of hepatic steatosis in nonalcoholic fatty liver disease. J Gastroenterol Hepatol. 2014;29:1470–6.

15. Karlas T, Petroff D, Sasso M, et al. Individual patient data meta-analysis of controlled attenuation parameter (CAP) technology for assessing steatosis. J Hepatol. 2017;66:1022–30.

16. Shi KQ, Tang JZ, Zhu XL, et al. Controlled attenuation parameter for the detection of steatosis severity in chronic liver disease: a meta-analysis of diagnostic accuracy. J Gastroenterol Hepatol. 2014;29:1149–58.

17. Gu Q, Cen L, Lai J, et al. A meta-analysis on the diagnostic performance of magnetic resonance imaging and transient elastography in nonalcoholic fatty liver disease. Eur J Clin Invest. 2021;51:e13446.

18. Broering D, Shawkat M, Albenmousa A, et al. Validating controlled attenuation parameter in the assessment of hepatic steatosis in living liver donors. PLoS ONE. 2021;16:e0251487.

19. Fujiwara Y, Kuroda H, Abe T, et al. The B-mode image-guided ultrasound attenuation parameter accurately detects hepatic steatosis in chronic liver disease. Ultrasound Med Biol. 2018;44:2223–32.

20. Tada T, Kumada T, Toyoda H, et al. Utility of attenuation coefficient measurement using an ultrasound-guided attenuation parameter for evaluation of hepatic steatosis: comparison with MRI-determined proton density fat fraction. Am J Roentgenol. 2019;212:332–41.

21. Tada T, Kumada T, Toyoda H, et al. Liver stiffness does not affect ultrasound-guided attenuation coefficient measurement in the evaluation of hepatic steatosis. Hepatol Res. 2020;50:190–8.

22. Kuroda H, Fujiwara Y, Abe T, et al. Two-dimensional shear wave elastography and ultrasound-guided attenuation parameter for progressive non-alcoholic steatohepatitis. PLoS ONE. 2021;16:e0249493.

23. Bende F, Sporea I, Şirli R, et al. Ultrasound-guided attenuation parameter (UGAP) for the quantification of liver steatosis using the controlled attenuation parameter (CAP) as the reference method. Med Ultrason. 2021;23:7–14.

24. Tada T, Kumada T, Toyoda H, et al. Attenuation imaging based on ultrasound technology for assessment of hepatic steatosis: a comparison with magnetic resonance imaging-determined proton density fat fraction. Hepatol Res. 2020;50:1319–27.

25. Yoo J, Lee JM, Joo I, et al. Reproducibility of ultrasound attenuation imaging for the noninvasive evaluation of hepatic steatosis. Ultrasonography. 2020;39:121–9.

26. Sugimoto K, Moriyasu F, Oshiro H, et al. The role of multiparametric US of the liver for the evaluation of nonalcoholic steatohepatitis. Radiology. 2020;296:532–40.

27. Lee DH, Cho EJ, Bae JS, et al. Accuracy of two-dimensional shear wave elastography and attenuation imaging for evaluation of patients with nonalcoholic steatohepatitis. Clin Gastroenterol Hepatol. 2021;19:797-805.e797.

28. Bae JS, Lee DH, Lee JY, et al. Assessment of hepatic steatosis by using attenuation imaging: a quantitative, easy-to-perform ultrasound technique. Eur Radiol. 2019;29:6499–507.

29. Chalasani N, Younossi Z, Lavine JE, et al. The diagnosis and management of non-alcoholic fatty liver disease: practice guideline by the American Association for the study of liver diseases, American College of Gastroenterology, and the American Gastroenterological Association. Hepatology. 2012;55:2005–23.

30. Tada T, Iijima H, Kobayashi N, et al. Usefulness of attenuation imaging with an ultrasound scanner for the evaluation of hepatic steatosis. Ultrasound Med Biol. 2019;45:2679–87.

31. Dietrich CF, Bamber J, Berzigotti A, et al. EFSUMB guidelines and recommendations on the clinical use of liver ultrasound elastography, update 2017 (long version). Ultraschall Med. 2017;38:e16–47.

32. Ferraioli G, Filice C, Castera L, et al. WFUMB guidelines and recommendations for clinical use of ultrasound elastography: part 3: liver. Ultrasound Med Biol. 2015;41:1161–79.

33. Bedossa P. Utility and appropriateness of the fatty liver inhibition of progression (FLIP) algorithm and steatosis, activity, and fibrosis (SAF) score in the evaluation of biopsies of nonalcoholic fatty liver disease. Hepatology. 2014;60:565–75.

34. DeLong ER, DeLong DM, Clarke-Pearson DL. Comparing the areas under two or more correlated receiver operating

characteristic curves: a nonparametric approach. Biometrics. 1988;44:837–45.

35. Eguchi Y, Hyogo H, Ono M, et al. Prevalence and associated metabolic factors of nonalcoholic fatty liver disease in the general population from 2009 to 2010 in Japan: a multicenter large retrospective study. J Gastroenterol. 2012;47:586–95.

36. Ekstedt M, Hagström H, Nasr P, et al. Fibrosis stage is the strongest predictor for disease-specific mortality in NAFLD after up to 33 years of follow-up. Hepatology. 2015;61:1547–54.

37. Angulo P. Nonalcoholic fatty liver disease. N Engl J Med. 2002;346:1221–31.